molecular pharmaceutics

Article

pubs.acs.org/molecularpharmaceutics

Effects of Solution Concentration on the Physicochemical Properties of a Polymeric Anticancer Therapeutic

Lili X. Peng,[†] Lei Yu,[‡] Stephen B. Howell,[§] and David A. Gough*,[†]

[†]Department of Bioengineering and [§]Moores Cancer Center, University of California, San Diego, La Jolla, California

[‡]Nitto Denko Technical Corporation, Oceanside, California

Supporting Information

ABSTRACT: Poly(γ-glutamyl-glutamate) paclitaxel (PGG−PTX) is a series of eighteen semiflexible polymer−drug constructs varying in PTX loading fraction (f_{PTX} of 0.18, 0.24, and 0.37) and spatial PTX arrangement (uniform, "even" and "random"; clustered, "clusters" and "ends"; concentrated, "ends" and "side"). Structural properties of PGG−PTX in dilute and concentrated conditions are determined from coarse-grained molecular dynamics (MD) simulations. Since PGG−PTX does not have a specific conformation, MD simulations were run until minimal structural deviations persisted. Root-mean-square deviation (RMSD) clustering was then used to determine the significant, unique characteristic conformations. Results show that dilute PGG−PTX undergoes a globule-to-filament transition with respect to increasingly denser PTX arrangements. While a similar transition is apparent in concentrated conditions, PGG−PTX tends to be more filamentous on the whole. PGG−PTX is also more rigid in concentrated conditions, and a higher PTX loading fraction leads to decreased flexibility. In general, the dilute "ends", "middle", and "side" PGG−PTX molecules at f_{PTX} = 0.18 and 0.24 prove to be the most efficaciously promising and are recommended for future biological testing. This study demonstrates the practicality of molecular modeling toward understanding structural behavior of an anticancer therapeutic in different solution concentrations.

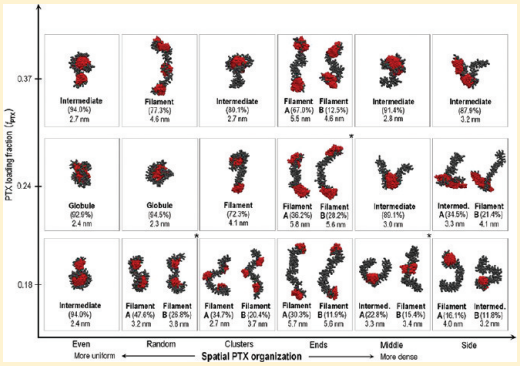

KEYWORDS: *polymer, modeling, coarse-grained, cancer therapeutic, conformation, solution concentration, paclitaxel, drug delivery*

INTRODUCTION

Modern cancer research has focused on the role of physicochemical properties of therapeutic nanoparticles in overcoming biological and physiological barriers that impede their delivery and localization to target tumors.[1,2] Y. Geng and G. Srinivas have argued that discoidal nanoparticles adhere more strongly to the walls of tumor endothelia than their spherical counterparts,[3−5] and P. Decuzzi has shown that longer blood circulation is associated with wormlike, filamentous polymers.[6,7] In addition, W. Jiang has demonstrated that 2−100 nm nanoparticles control basic intracellular signaling processes necessary for tumor cell functions, such as apoptosis.[8] Finally, S. Takeoka has theorized that higher particle flexibility increases the number of interactions to cell surfaces and subsequently improves binding to tumor cells.[9] Collectively these observations suggest the shape, size, and flexibility as a central basis for the clinical design of an anticancer therapeutic.

This study explores the shape, size, and flexibility of poly(γ-glutamyl-glutamate) paclitaxel (PGG−PTX), an anticancer polymer−drug construct in preclinical evaluation. Paclitaxel (Taxol, $C_{47}H_{51}NO_{14}$) is a mitotic inhibitor commonly used in breast, ovarian, and lung cancer chemotherapy.[10−12] Paclitaxel alone is therapeutically effective, but its poor solubility severely limits its use in natural form. Furthermore, nonspecific accumulation of paclitaxel in normal tissue results in elevated cytotoxicity levels that subsequently hinder paclitaxel from reaching its maximum therapeutic potential.[13] Therefore, to improve its efficacy, paclitaxel is covalently conjugated to poly(γ-glutamyl-glutamate) (PGG), a hydrophilic and biocompatible polymer that has been shown to improve solubility, increase circulation half-life, and enhance selectivity of paclitaxel to target tumors.[14−16] Combination of the flexible PGG and rigid PTX entities generates a semiflexible, more water-soluble PTX derivative whose physicochemical properties differ from those of the rigid paclitaxel itself.

In preclinical studies, the safety and effectiveness of PGG−PTX is rigorously evaluated through an iterative, trial-and-error process of pharmacokinetics, pharmacodynamics, ADME, and toxicity testing on laboratory animals. This is a significantly time-consuming and resource-intensive process that can take up to seven years. Given the urgency of cancer patients, there is a need for new methodologies to facilitate this process.[17] Computer simulations can offer theoretical insight into physicochemical properties of anticancer therapeutics that is

Received: April 29, 2011
Revised: August 2, 2011
Accepted: October 11, 2011
Published: October 11, 2011

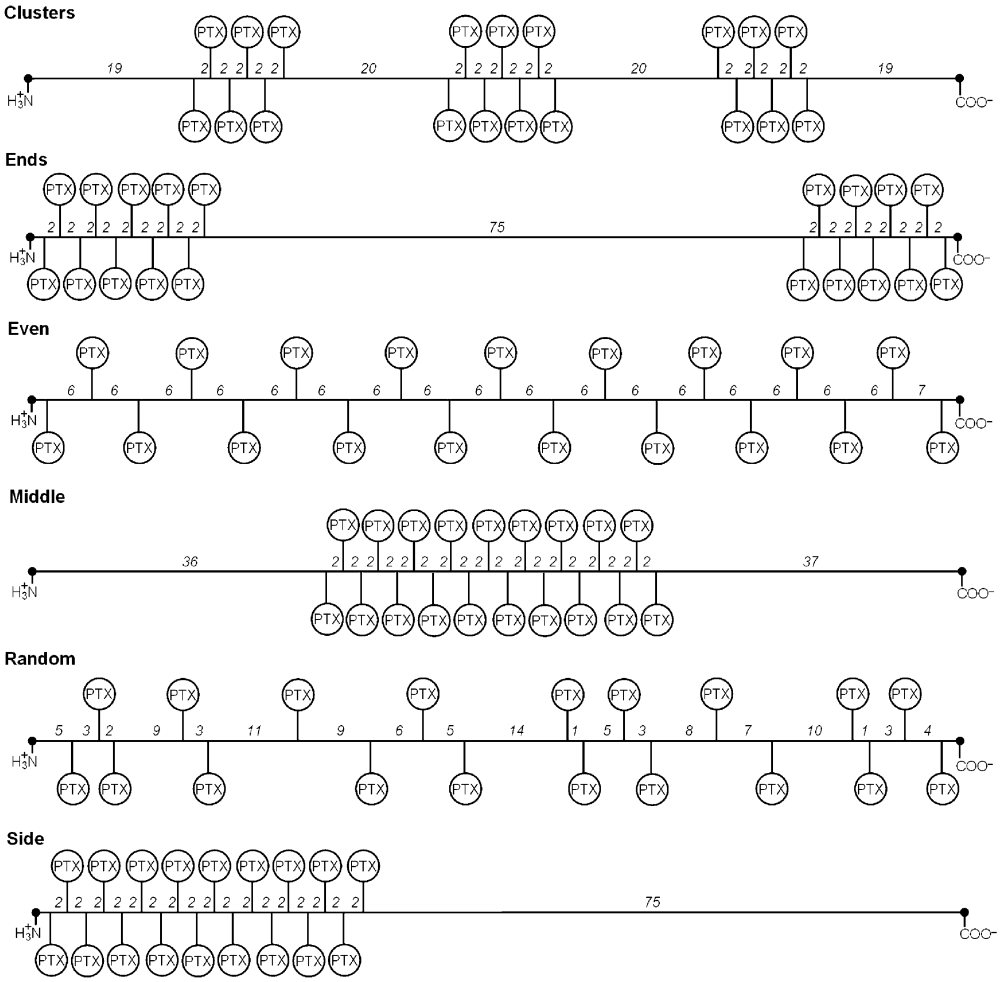

Figure 1. Abstract representation of the spatial PTX arrangements on the PGG backbone for f_{PTX} = 0.24 molecules. Each PGG−PTX molecule is composed of 130 poly-(γ-glutamyl-glutamate) monomers and 19 PTX molecules. Figure shows how 19 PTX molecules are covalently attached to the PGG backbone in six different fashions: "even" (each PTX is spaced an equal number of residues apart along PGG), "random" (all PTX molecules located in random positions), "clusters" (3 PTX groups with 4−5 PTX per group, spaced an equal number of residues apart), "ends" (2 PTX groups with 9 or 10 PTX each, located at both ends), "middle" (all PTX molecules positioned in the middle), and "side" (all PTX molecules located at the amino terminus end). Numbers between residues denote number of repeating GG residues that are not amino- or carboxyl-termini GG residues. The amino- and carboxyl-termini GG residues are represented by black dots at the ends of each line. The abstract representations for the f_{PTX} = 0.18 and 0.37 molecules are shown in Figures S1 and S2, respectively, in the Supporting Information. (Adapted from Peng et al.[21].)

difficult to access experimentally. The resulting information can be further used to design meaningful experiments, and streamline and improve cost-effectiveness of preclinical testing. In this study, we utilize computer simulations to determine how two primary properties, PTX loading fraction (f_{PTX}) and spatial PTX arrangement on the PGG backbone, impact macromolecular structural features of PGG−PTX, namely, as shape, size, and flexibility. The existing PGG−PTX formulations are categorized by PTX loading fraction, defined as

$$f_{PTX} = \frac{MW_{PTX}}{MW_{PGG-PTX}} \quad (1)$$

where MW_{PTX} is the molecular weight of all PTX entities on a PGG−PTX molecule and $MW_{PGG-PTX}$ is the molecular weight of the PGG−PTX molecule. Each PGG−PTX formulation comprises a 130-mer PGG backbone coupled with 12 PTX molecules (f_{PTX} = 0.18), 19 PTX molecules (f_{PTX} = 0.24), or 26 PTX molecules (f_{PTX} = 0.37). For the molecular models, the spatial PTX arrangements were defined as uniform ("even" and "random"), clustered ("clusters" and "ends"), and dense ("middle" and "side") patterns for each PTX loading fraction, resulting in an array of eighteen unique PGG−PTX molecules, as shown in Figure 1.

■ MODELING APPROACH

Prior to modeling, the initial PGG−PTX structure was in question. In conventional molecular dynamics (MD) simulations, a starting structure is taken from the Protein Data Bank (PDB), an online repository of biomolecules whose three-dimensional structures are determined from X-ray crystallography and nuclear magnetic resonance spectroscopy.[18−20] Since there was no PDB structure of PGG−PTX available, circular dichroism (CD) spectroscopy was used to approximate its initial structure.

In vivo conditions were considered by taking into account characteristics of the medium surrounding PGG−PTX. For intravenous injection into the bloodstream, the aqueous formulation of PGG−PTX is dissolved in pure water. Although the initial loading dose and volume of distribution of PGG−PTX were not available at the commencement of this study, we

dx.doi.org/10.1021/mp2002208 | *Mol. Pharmaceutics* 2012, 9, 37−47

Table 1. Box Dimensions and Volumes for PGG−PTX Molecules in Concentrated Conditions

	f_{PTX} = 0.18		f_{PTX} = 0.24		f_{PTX} = 0.37	
	dimens (nm × nm × nm)	vol (nm^3)	dimens (nm × nm × nm)	vol (nm^3)	dimens (nm × nm × nm)	vol (nm^3)
even	19.9 × 8.5 × 18.4	3135.0	21.9 × 10.3 × 12.8	2878.9	24.1 × 9.4 × 11.7	2656.0
random	20.4 × 8.8 × 15.0	2703.1	19.9 × 15.3 × 8.1	2464.9	19.8 × 8.3 × 17.2	2830.8
clusters	25.3 × 13.4 × 10.2	3655.6	20.6 × 9.3 × 12.4	2617.7	20.2 × 7.9 × 12.1	1913.7
ends	24.4 × 7.6 × 15.7	2892.3	23.6 × 10.4 × 10.5	2577.8	25.2 × 9.5 × 14.1	2617.5
middle	24.0 × 5.9 × 12.5	1768.0	26.6 × 8.1 × 12.7	2750.2	14.9 × 13.6 × 13.3	2617.7
side	22.2 × 7.8 × 16.4	2849.2	24.7 × 7.0 × 11.6	2017.8	24.6 × 6.4 × 8.5	1333.5

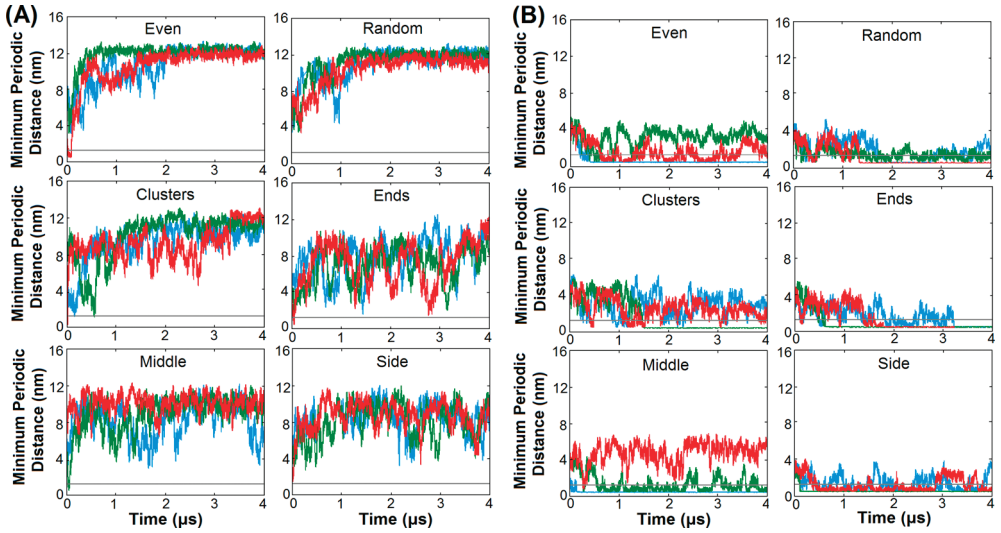

Figure 2. Minimum periodic distance trajectories for PGG−PTX molecules. Trajectories correspond to f_{PTX} = 0.18 (blue), 0.24 (green), and 0.37 (red) for (A) dilute and (B) concentrated conditions. Grey line indicates long-range cutoff of 1.2 nm.

surmised that the concentration of PGG−PTX is initially high when it enters the bloodstream but eventually decreases to a very dilute solution until accumulation in tissues and renal clearance. To depict how PGG−PTX behaves in both conditions, a PGG−PTX molecule is encapsulated within a unit cell whose size is manipulated to represent dilute and concentrated conditions. Periodic boundary conditions (PBC) are often invoked to simulate a large system by modeling a small unit cell far from the edge; a species passes through a side of the box only to reappear on the opposite side and interacts with its periodic image. When PBC are applied for a unit cell large enough such that the molecule does not interact with its periodic image, dilute conditions are signified. On the other hand, concentrated conditions can be induced by setting a unit cell small enough to enclose a molecule so that interactions between periodic PGG-PTX images occur. Traditionally, in MD simulations, the box size is set to minimize periodic interactions in order to determine the natural conformation of a molecular species. However, this study focuses on exploring the effects of environmental conditions, namely, solution concentration, on structural properties of a polymer−drug conjugate.

Once molecular simulations were commenced, deciding when to end was the next challenge. Due to its semiflexibility, PGG−PTX is not expected to exist as a static structure but as a range of similar shapes. Therefore, simulations were run until minimal movement existed at the molecule level, a *statistical equilibrium* at which PGG−PTX exists as a dynamic ensemble of statistically related conformations.

COMPUTATIONAL MODELING

Simulation Parameters. The governing mathematical equations describing the coarse-grained (CG) MD simulations, mapping of all-atom (AA) models to CG models, and CG parametrization of PGG−PTX molecules have been described.[21] For dilute conditions, each PGG−PTX molecule was solvated in the center of a 20 nm × 20 nm × 20 nm box and surrounded by explicit CG water beads. For concentrated conditions, the unit cell was adjusted to ensure that physical interactions between periodic PGG−PTX images occurred (see Table 1). For both conditions, to maintain system neutrality, the negative charges imparted by the glutamyl-glutamate residues required the replacement of 248, 241, and 234 CG water beads with sodium ions for the f_{PTX} = 0.18, 0.24, and 0.37 systems, respectively.

CG MD simulations were run using GROMACS 4.0.3.[22] The NPT ensemble (the number of particles N, pressure P, and temperature T were all fixed) was applied for the simulations; the temperature was kept at 310 K with a coupling constant of τ_T = 0.1 ps; and the pressure was weakly coupled to 1 bar with a relaxation time of τ_P = 0.5 ps. The cutoff length for the nonbonded interactions was r_{cut} = 1.2 nm. Lennard-Jones and Coulombic forces were considered for r_{cut} < 0.9 nm and r_{cut} < 1.2 nm, respectively, and the latter was computed every time step for 1.0 nm and once every 10 time steps for 0.9 nm < r_{cut} < 1.2 nm. The time step in the leapfrog integration scheme was 5 fs. The energies, coordinates and velocities were written every 0.5 ps. MD simulations were run until a statistical equilibrium was reached at 1 μs. The time scale was scaled up by a factor of 4 because coarse-grained dynamics are faster than all-atom

dx.doi.org/10.1021/mp2002208 | *Mol. Pharmaceutics* 2012, 9, 37−47

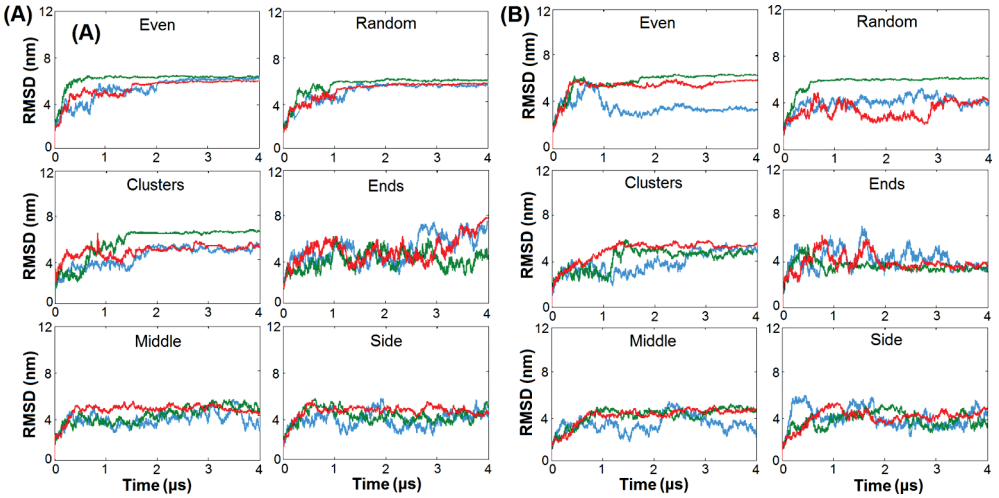

Figure 3. RMSD trajectories for PGG−PTX molecules. Trajectories correspond to f_{PTX} = 0.18 (blue), 0.24 (green), and 0.37 (red) for (A) dilute and (B) concentrated conditions.

dynamics, due to the smoothness of the CG interactions. This factor of 4 is based on the speedup in the diffusional dynamics of CG water as compared to AA water. Therefore, the simulation time scale was scaled up by a factor of 4 resulting in an effective time of 4 μs.[23−25]

Validation of Periodic Interactions. The *g_mindist* module of GROMACS 4.0.3 was used to analyze the minimum distance between periodic images throughout the 4 μs trajectory. The long-range cutoff of 1.2 nm was used to distinguish between dilute and concentrated conditions. Dilute conditions are characterized by minimum periodic interactions higher than 1.2 nm, and concentrated conditions by minimum periodic distances below 1.2 nm. The minimum periodic distance is above 1.2 nm for all PGG−PTX molecules (see Figure 2A), so this lack of periodic interactions confirms that conditions are met. For the f_{PTX} = 0.24 "clusters" and f_{PTX} = 0.37 "ends" molecules, the minimum periodic distance nears 1.2 nm at 0.6 ns and 2.8 ns, respectively, but for the majority of the trajectory, their minimum periodic distances values hover between 4 and 12 nm, well above 1.2 nm. Also, Figure 2B shows that the minimum periodic distance values fall below 1.2 nm, suggesting concentrated PGG−PTX conditions.

RMSD CLUSTERING

Root-mean-squared deviation (RMSD) clustering is a quantitative method used to determine the conformation of a molecular species.[21,26] In RMSD clustering, all conformations accessed during a simulation are categorized into clusters based on structural similarity. Then, for each cluster, a structure from the MD trajectory closest to the geometrical average of all conformations accessed during the MD simulation was regarded as the characteristic conformation.

RMSD clustering analysis of PGG−PTX molecules was done using the *g_cluster* module of GROMACS 4.0.3. First, the RMSD cutoff was optimized to meet the following criteria: (1) the total number of clusters was approximately 40, (2) 90% of the trajectory was contained in clusters fewer than 40, and (3) very few clusters included one configuration. (Figure S3 in the Supporting Information shows a sample graph of the RMSD cutoff length vs number of clusters generated for the f_{PTX} = 0.18 "clusters" molecule in dilute conditions, whose RMSD cutoff length of 0.658 nm corresponds to 41 clusters. In addition, the optimized RMSD cutoff distances for PGG−PTX in dilute and concentrated conditions are provided in Tables S1 and S2 in the Supporting Information, respectively.) Since a PGG−PTX molecule can have up to ∼40 clusters, only those that are statistically significant, or occupying at least 10% of the 4 μs trajectory, were respected. A PGG−PTX molecule can also have multiple significant characteristic conformations, as long as they are unique. The uniqueness for each significant characteristic conformation was evaluated using the RMSD Calculator of Visual Molecular Dynamics 1.8.6.[27] If the RMSD between each significant characteristic conformation were greater than twice the RMSD cutoff, then the significant conformation(s) was/were deemed unique (see Table S1 in the Supporting Information). A PDB structure was extracted from each significant, unique characteristic conformation.

DENSITY ANALYSIS

It was of interest to determine how PTX loading fraction and spatial PTX arrangement influence the packing of a PGG−PTX molecule and its respective PGG and PTX residues. The radial distribution function $g(r)$ is often used to characterize the structural arrangement of a molecular species.[28] For two species A and B, the $g_{AB}(r)$ is defined as

$$g_{AB}(r) = \frac{\rho_{AB}(r)}{\rho_{B,local}} \quad (2)$$

where $\rho_{AB}(r)$ is the particle density of species B at a distance r from species A and $\rho_{B,local}$ is the local density of species B at a maximum distance r_{max} from species A. While $g(r)$ analysis is routinely used in biomolecular MD simulations, in this study, the different box volumes for PGG−PTX molecules in concentrated conditions result in different $\rho_{B,local}$ values. To account for the various local densities, the density of a PGG−PTX molecule from its center-of-mass (COM), $\rho_{AB}(r)$, was used to describe its structure in concentrated conditions, and for consistency, in dilute conditions. Using the definition of the radial distribution function, the density of a PGG-PTX molecule its COM can then be determined from multiplying $g_{AB}(r)$ and $\rho_{B,local}$: $\rho_{AB}(r) = g_{AB}(r) \times \rho_{B,local}$. The local density of a PGG−PTX molecule can be determined from its molecular mass and simulation box size (see Table S3 and Scheme S1 in

dx.doi.org/10.1021/mp2002208 | *Mol. Pharmaceutics* 2012, 9, 37−47

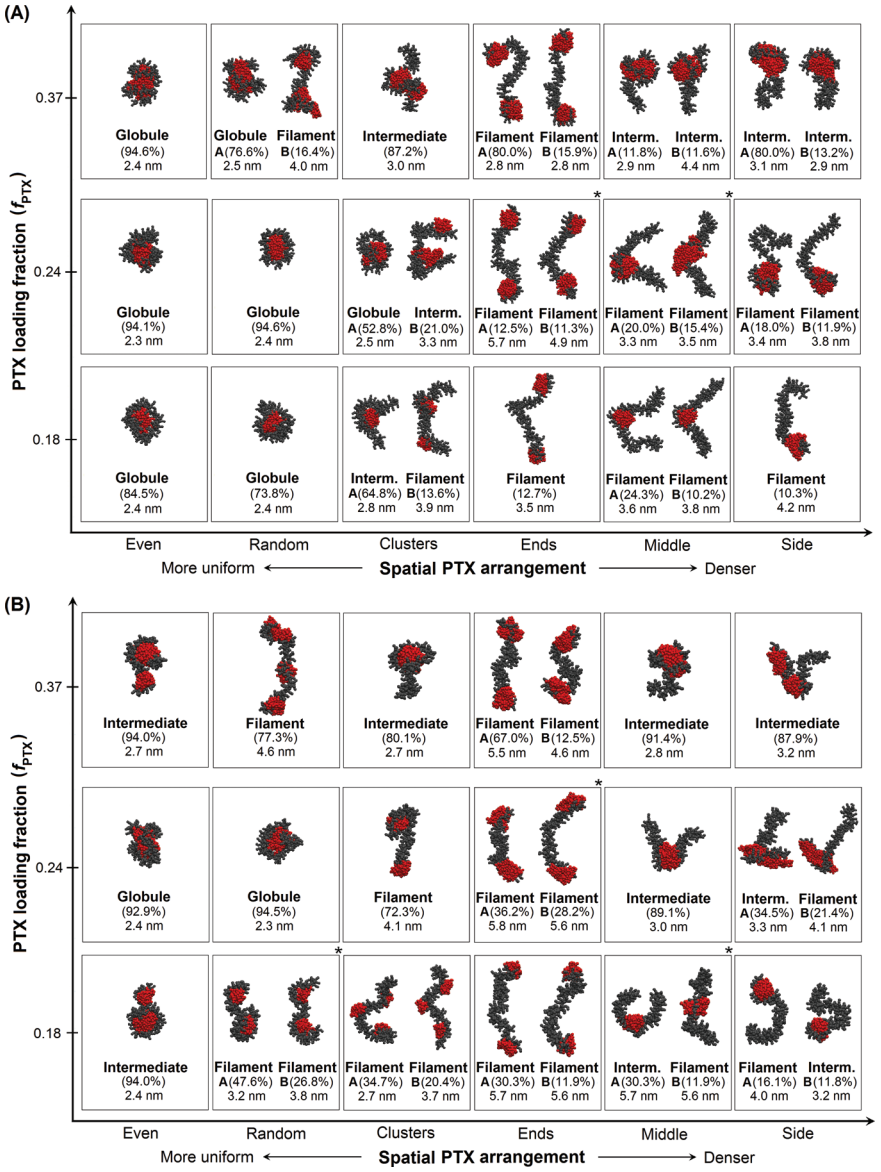

Figure 4. Significant, unique characteristic conformations of PGG–PTX molecules in (A) dilute and (B) concentrated conditions as a function of PTX loading fraction and spatial PTX organization. Each structure shows the PGG (grey) and PTX (red) residues. The radius of gyration is also noted for each characteristic conformation, along with the percentage (%) trajectory occupancy corresponding to the particular characteristic conformation for the 4 μs MD trajectory. Molecules with more than two characteristic conformations are denoted with an asterisk (*); the top two conformations are shown, and the remaining conformation(s) are shown in Figure S4 in the Supporting Information.

the Supporting Information). It is important to emphasize that the COM does not necessarily correspond to the geometric center, particularly for irregularly shaped molecules, and the COM tends to be prominent at the more massive end. The *g_rdf* module was used to extract the $g_{AB}(r)$ values; species A refers to the center-of-mass of a PGG–PTX molecule and species B the overall PGG–PTX molecule. Plots for the $\rho_{AB}(r)$ values of PGG–PTX molecules and their respective PGG and PTX residues are shown in Figures 5–7.

RESULTS AND DISCUSSION

RMSD Values. Figure 3 shows the RMSD trajectories for PGG–PTX molecules in dilute and concentrated conditions. Similar behavior is witnessed under both conditions. All RMSD curves rose to ~4–6 nm by 4 μs, with some attaining nearly 8 nm. These values are high, but given the relatively large size of PGG–PTX, the systems are adequately stabilized. For some molecules such as f_{PTX} = 0.24 "even", f_{PTX} = 0.24 "random", and f_{PTX} = 0.37 "random", the RMSD values for concentrated conditions are slightly lower than those for dilute conditions, indicating smaller deviation from the starting structures. For dilute conditions, the "even", "random", and "clusters" systems exhibit flatter plateaus between 2 and 4 μs than do the "ends", "middle", and "side" systems, suggesting that PGG–PTX molecules with more concentrated PTX arrangements fluctuate more than do those with denser PTX arrangements. Higher RMSD fluctuations also indicate higher molecular flexibility, which is further discussed in "Flexibility of a PGG–PTX Molecule."

Shape and Structure of a PGG–PTX Molecule. Figure 4 shows the significant, unique characteristic conformations of PGG–PTX molecules in dilute and concentrated conditions. The geometry of each molecule is designated as a filamentous (threadlike and wormlike in shape), globular (round in shape),

dx.doi.org/10.1021/mp2002208 | *Mol. Pharmaceutics* 2012, 9, 37–47

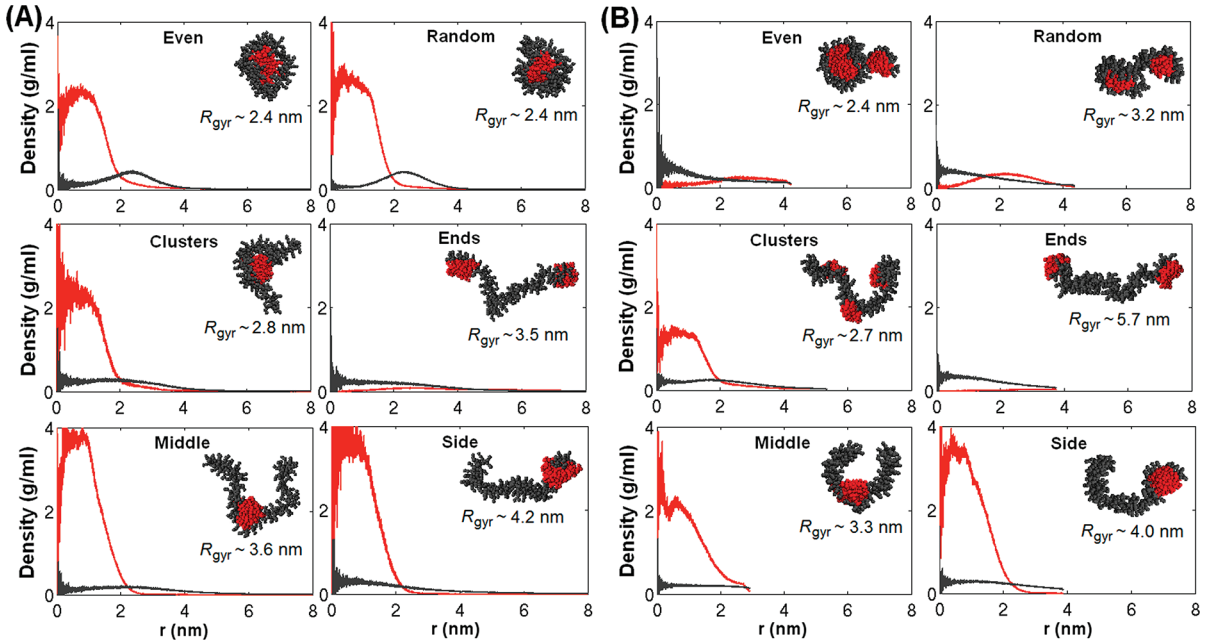

Figure 5. Density profiles f_{PTX} = 0.18 PGG-PTX systems. Trajectories correspond to the (A) dilute and (B) concentrated conditions for the PGG residues (grey) and PTX (red) residues. For each system, the unique characteristic conformation of highest significance is shown at the upper right-hand corner. Note: the center-of-mass (r = 0) does not necessarily refer to the geometric center but where the molecule is highest in mass.

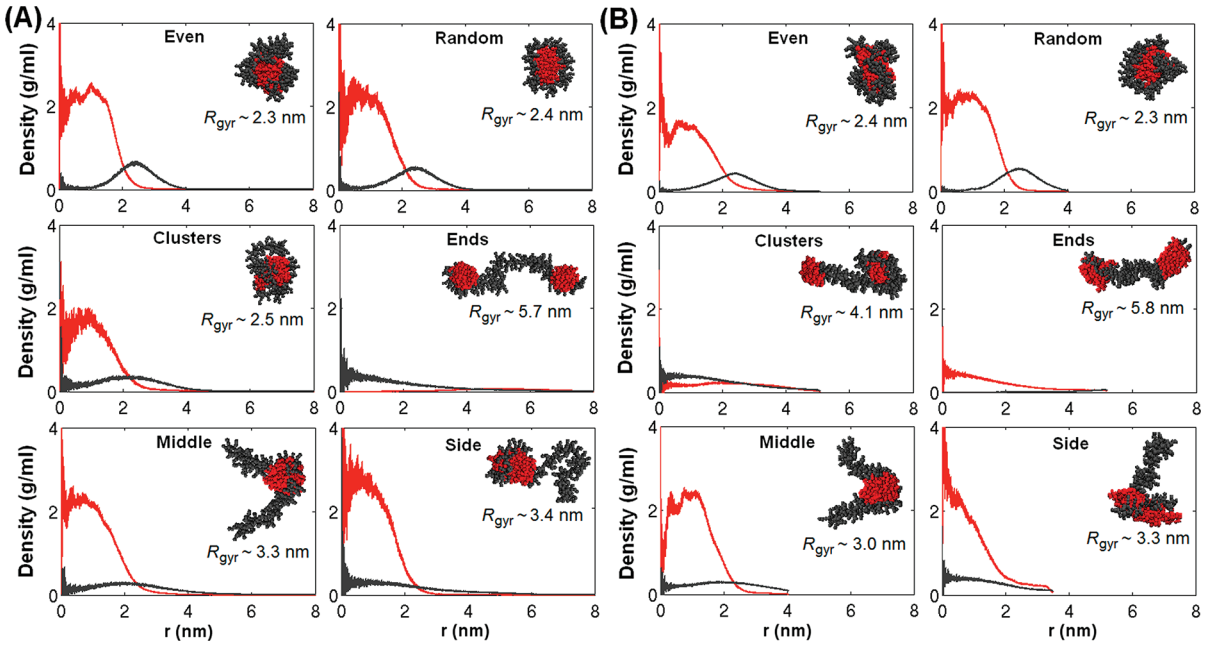

Figure 6. Density profiles f_{PTX} = 0.24 PGG-PTX systems from center-of-mass. Trajectories correspond to the (A) dilute and (B) concentrated conditions for the PGG residues (grey) and PTX (red) residues. For each system, the unique characteristic conformation of highest significance is shown at the upper right-hand corner.

and/or intermediate (having filamentous and globular features). Also supplemented to describe morphology are the structural PGG and PTX densities of the PGG-PTX molecules in dilute and concentrated conditions in Figures 5−7. A filament is characterized by low PGG and PTX densities from r = 0 nm to $r = r_{max}$, such as the "ends" PGG-PTX molecule in both dilute and concentrated conditions at all three PTX loading fractions. On the other hand, a PGG−PTX molecule with significantly higher PGG densities at r = 0 than at $r = r_{max}$ and whose PTX density peaks somewhere between r = 0 and $r = r_{max}$ is a globule, as exhibited by the "even" and "random" systems in dilute conditions. The density plot for an intermediate geometry is similar to that of a globule in that the PGG density values are highest at r = 0 nm and gradually decreases as $r \rightarrow r_{max}$. However, the apparent plateau from 0 nm < r < 1.5 nm in the PGG density plot of a globule is not prevalent in the PGG density plot of an intermediate. For example, in Figure 6, the PGG density for the f_{PTX} = 0.37 "middle" in dilute conditions peaks at r = 0 but decreases more

dx.doi.org/10.1021/mp2002208 | *Mol. Pharmaceutics* 2012, 9, 37−47

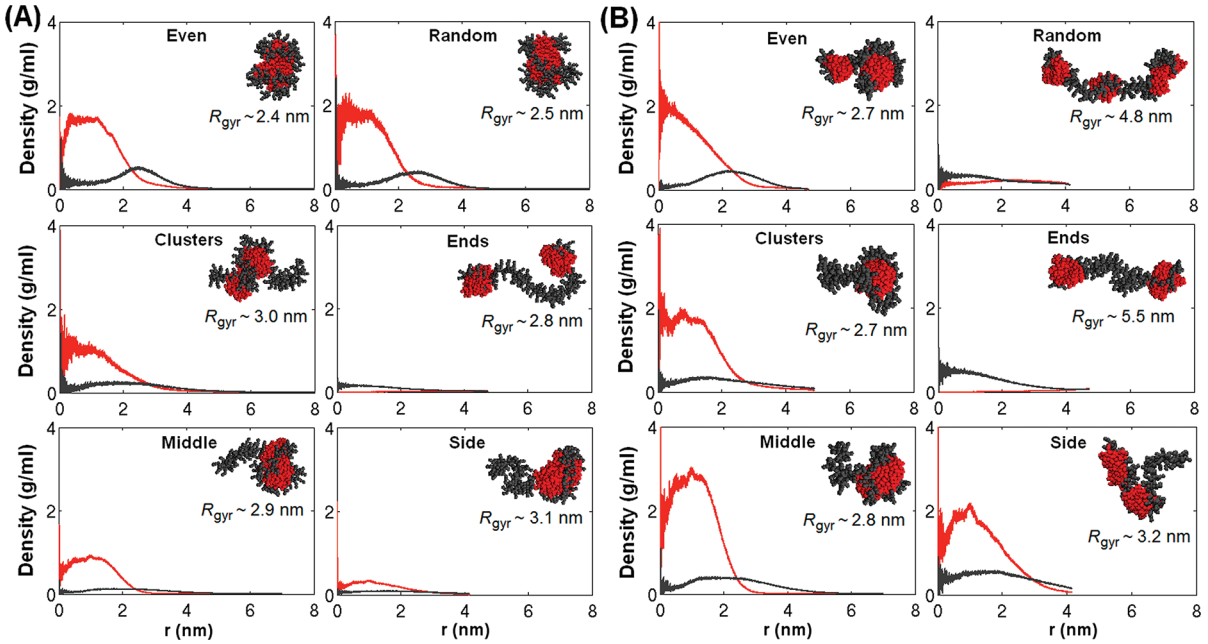

Figure 7. Density profiles f_{PTX} = 0.37 PGG-PTX systems center-of-mass. Trajectories correspond to the (A) dilute and (B) concentrated conditions for the PGG residues (grey) and PTX (red) residues. For each system, the unique characteristic conformation of highest significance is shown at the upper right-hand corner.

sharply from 0 nm < r < 1.5 nm than does the PGG density of the f_{PTX} = 0.37 "even" in dilute conditions.

Dilute Conditions. As apparent in Figure 4, for dilute conditions, a PGG−PTX molecule is globular at the most uniform PTX arrangements ("even" and "random") and adopts more filamentous behavior as the PTX arrangement becomes denser ("middle" and "side"). PGG−PTX molecules with clustered PTX distributions ("ends" and "clusters") are defined by combination of globular, filamentous, and intermediate shapes. This intriguing pattern is most likely attributed to the hydrophobic driving force among intramolecular PTX molecules. For instance, the uniform PTX arrangement causes the entire "even" or "random" molecule to collectively self-assemble into a globule in which the hydrophobic PTX molecules are located in the inner rigid core, where they are shielded from the aqueous solvent by their hydrophilic PGG backbone. These results are further supported by Figures 5A, 6A, and 7A (top two panels), which shows that, as $r \rightarrow 0$, PTX density increases while PGG density decreases. PGG density also eventually peaks at a certain distance between r = 0 and $r = r_{max}$ surrounding the PTX core. For denser arrangements, loading of PTX molecules onto a more confined region of the PGG backbone limits intramolecular PTX self-assembly to only that region. The lengthy, conjugated portion of the flexible PGG backbone is then free to move about, which is responsible for the filamentous "side" and "middle" shapes in dilute conditions. Since the clustered PTX arrangement is an intermediate between uniform and dense PTX arrangements, the dilute "clusters" and "ends" PGG−PTX molecules exhibit globular and filamentous traits.

Also in dilute conditions, the presence of the intermediate morphology becomes more pronounced with increasing PTX loading fraction. At f_{PTX} = 0.18 and 0.24, only the "clusters" molecule exhibits intermediate behavior, but at f_{PTX} = 0.37, intermediate shapes are present in the "clusters", "middle", and "side" molecules. Again, this trend is a likely consequence of the hydrophobic driving force among PTX molecules. A higher PTX loading fraction will result in stronger hydrophobic interactions, subsequently forming a tightly packed core of PTX molecules. The density profiles in Figures 5A, 6A, and 7A further support this hypothesis. At f_{PTX} = 0.18 and 0.24, Figures 5A and 6A show that the PTX residues in the dilute "clusters", "middle", and "side" molecules are densely packed near r = 0 nm of PGG−PTX. However, at f_{PTX} = 0.37 in Figure 7A, the PTX density near r = 0 nm decreases considerably. This PTX bundle is morphologically similar to the PTX core in the "even" and "random" molecules, only that the "clusters", "middle", and "side" molecules have unconjugated PGG tails responsible for their wormlike nature, thus contributing to their intermediate geometry.

Concentrated Conditions. At concentrated conditions, the globule-to-filament transition with respect to denser spatial PTX arrangements is still prevalent but not as significant as that of dilute conditions. For instance, while globules are present at all three PTX loading fractions for the "even" and "random" molecules in dilute conditions, Figure 4B shows that this shape is witnessed only at f_{PTX} = 0.24 for the molecules with uniform PTX arrangements in concentrated conditions. Also, as aforementioned, the "clusters" and "ends" molecules are characterized by globular, intermediate, and filamentous shapes. However, in concentrated conditions, these molecules exist only as intermediates and filaments. Similar to dilute conditions, the "middle" and "side" PGG−PTX molecules have intermediate and filamentous shapes, but the intermediate is more common in concentrated conditions, whereas the filament is more prevalent in dilute conditions. In addition, the evidence of periodic interactions in Figure 2 suggests that the shape of a PGG−PTX molecule is skewed by interactions with neighboring PGG−PTX molecules. In other words, the filamentous morphology of f_{PTX} = 0.18 "even", f_{PTX} = 0.37 "even", f_{PTX} = 0.37 "random", and f_{PTX} = 0.24 "clusters" molecules is caused by the intermolecular PTX interactions among neighboring PGG−PTX molecules. Figure S5 in the Supporting Information shows the periodic interactions among

dx.doi.org/10.1021/mp2002208 | *Mol. Pharmaceutics* 2012, 9, 37−47

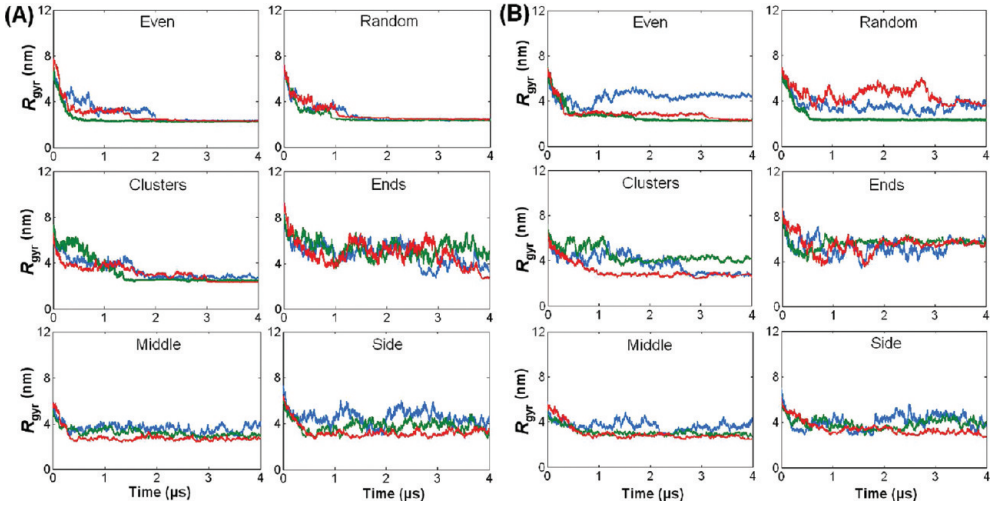

Figure 8. Radius of gyration trajectories for PGG−PTX molecules. Trajectories correspond to f_{PTX} = 0.18 (blue), 0.24 (green), and 0.37 (red) for (A) dilute and (B) concentrated conditions.

PTX molecules of neighboring PGG−PTX molecules. The minimum periodic values below 1.2 nm in the f_{PTX} = 0.18 "even", f_{PTX} = 0.37 "even", f_{PTX} = 0.37 "random", and f_{PTX} = 0.24 "clusters" molecules suggest that the dominance of intermolecular PTX interactions over intramolecular PTX interactions leads to more filamentous morphologies. In dilute conditions, the dominance of intramolecular PTX interactions over intermolecular PTX interactions results in more globular PGG-PTX molecules.

This globule-to-filament transition is not always witnessed in molecules exhibiting intermolecular PTX interactions in concentrated conditions. For instance, the minimum periodic distance values drop below 1.2 nm for the "ends" molecule, but in dilute conditions it is a filament at all PTX loading fractions. The two PTX groups on the "ends" molecule are loaded just far enough apart on PGG to prevent intramolecular hydrophobic self-assembly that is witnessed in the other five PTX arrangements. In other words, the "ends" morphology is influenced mostly by spatial PTX arrangement, rather than PTX loading fraction or solution concentration.

Size of a PGG−PTX Molecule. Figure 8 shows the radius of gyration (R_g) trajectories for PGG−PTX molecules in dilute and concentrated conditions. Most molecules start out at approximately $R_g \sim 6-8$ nm and decrease to nearly half their original size ($R_g \sim 3-4$ nm) by 4 μs. The size of each PGG−PTX molecule is related to its molecular size; molecules with higher R_g values tend to be filaments, and molecules with lower R_g values, globules.

For dilute conditions, the "even", "random", and "clusters" molecules have slightly lower R_g values than do the "ends", "middle", and "side" molecules, although the difference of ∼1−2 nm is minimal. This size difference is consistent with the morphology of the PGG−PTX molecules; the globular shapes of the "even", "random", and "clusters" systems is smaller than the filamentous "ends", "middle", and "side" systems.

A PGG-PTX molecule is slightly larger in concentrated conditions than in dilute conditions, as suggested by the overall increase in R_g values for the "even" molecule at f_{PTX} = 0.18, "random" molecules at f_{PTX} = 0.18 and 0.37, and "ends" molecules at f_{PTX} = 0.18, 0.24, and 0.37. This behavior also agrees with the higher prevalence of filamentous shapes in concentrated conditions. Since a filament occupies more space than a globule, it is reasonable that the filamentous PGG−PTX molecules have higher R_g values than globular PGG−PTX molecules.

Flexibility of a PGG−PTX Molecule. The flexibility of each PGG−PTX molecule was assessed by the number of unique characteristic conformations and their degree of significance as indicated by % trajectory occupancy. A molecule with more significant, unique characteristic conformations indicates higher flexibility, and vice versa. For instance, a molecule characterized by one significant, unique characteristic PGG-PTX conformation occupying 80% of the 4 μs trajectory is less flexible than one with three significant, unique characteristic conformations each with 20% trajectory occupancy. For this study, a unique, characteristic conformation was considered significant if its % trajectory occupancy > 10%.

Dilute Conditions. In dilute conditions, the "even" and "random" molecules have one characteristic conformation with significant % trajectory occupancies (80−90%), suggesting low flexibility. PGG−PTX molecules with clustered and dense PTX arrangements are more flexible, as evidenced by two or three significant, unique characteristic conformations with % trajectory occupancies lower than those of the "even" and "random", indicating higher flexibility. Out of all PGG−PTX molecules, the f_{PTX} = 0.18 "ends" and "side" molecules are the most flexible, since each has a single characteristic conformation with a meager 10−12% trajectory occupancy. The f_{PTX} = 0.24 "ends", "middle", and "side" and f_{PTX} = 0.37 "middle" are comparable in flexibility. In general, increasing PTX loading fraction causes the molecular flexibility to decrease. At f_{PTX} = 0.37, 5 out of 6 molecules have unique characteristic conformations with at least 65% trajectory occupancy, as compared to the 3 out of 6 molecules exhibiting such % trajectory occupancy at f_{PTX} = 0.24 and 0.18. The increasing number of rigid PTX molecules on the PGG backbone is most likely responsible for this behavior.

Concentrated Conditions. In concentrated conditions, PGG−PTX molecules are usually more rigid than their dilute counterparts. Unlike the f_{PTX} = 0.18 "ends" and "side" molecules in dilute conditions, no molecule in concentrated conditions is characterized by a unique characteristic conformation with a very low % trajectory occupancy. In fact, 10 out of 18 PGG−PTX molecules are characterized by a single

dx.doi.org/10.1021/mp2002208 | *Mol. Pharmaceutics* 2012, 9, 37−47

significant, unique characteristic conformation with at least 70% trajectory occupancy. In dilute conditions, only six molecules fit this criterion. What is similar to dilute conditions is that the "even" and "random" molecules are the most rigid, for % trajectory occupancies are above 90%, and the most flexible molecules tend to have clustered and concentrated PTX arrangements. An increase in the PTX loading fraction causes a marked decrease in flexibility of a PGG-PTX molecule. Five out of six molecules have at least 65% trajectory occupancy at f_{PTX} = 0.37; 4 out of 6 at f_{PTX} = 0.24; and 1 out of 6 at f_{PTX} = 0.18. The f_{PTX} = 0.18 molecules have the highest number of significant, unique characteristic conformations, suggesting highest flexibility among all three PTX loading fractions. This general behavior is most likely attributed to the periodic interactions among adjacent PGG-PTX molecules. Due to the lack of periodic interactions in dilute conditions, molecular flexibility can only be influenced by PTX loading fraction and spatial PTX arrangement. The presence of periodic interactions in concentrated conditions is an additional limiting factor on PGG-PTX flexibility.

As shown in Figure 4, the "even" and "random" molecules usually are characterized by one characteristic conformation that occupies nearly the entire MD trajectory (80−90%). On the contrary, the "middle" and "side" systems exhibit multiple characteristic conformations that each occupy a smaller portion of the MD trajectory. Therefore, PGG−PTX systems with uniform PTX arrangements are less flexible, while the systems with dense PTX arrangements are more flexible. The PGG−PTX systems with clustered PTX arrangements ("clusters" and "ends") seem to exhibit an intermediate level of flexibility in-between the flexibility of the uniform and concentrated PGG-PTX systems. For example, the f_{PTX} = 0.37 "clusters" system is characterized by one characteristic conformation that occupies nearly 90% of its MD trajectory, while the "ends" systems at f_{PTX} = 0.24 and f_{PTX} = 0.37 are characterized by 2−4 characteristic conformations that occupy only 11% of their MD trajectories. Overall, the more concentrated the PTX arrangement on the PGG backbone, the more flexible the PGG−PTX molecule.

It is also noteworthy that, while the "ends" and "side" systems at f_{PTX} = 0.18 are characterized by one characteristic conformation, their corresponding % trajectory occupancies are relatively low (10−13%). Each characteristic conformation corresponded to the only significant *and* unique cluster obtained from the RMSD clustering analysis. There were other unique clusters that occupied the remainder of the 4 μs MD trajectory, but they were only present for less than 10% (data not shown). Since those unique clusters were not considered significant in the RMSD clustering analysis, their characteristic conformations were not considered in this study. Since the "ends" and "side" molecules at f_{PTX} = 0.18 are actually composed of multiple unique clusters that were not considered significant, these systems sample a wider range of conformations as compared to the other systems. Therefore, the "ends" and "side" systems at f_{PTX} = 0.18 are the most flexible PGG−PTX molecules.

For the "even" and "random" systems, the uniform PTX distribution causes the entire PGG−PTX molecule to self-assemble into a globule, where PTX molecules are located in the core. The strong hydrophobic driving force causes the entire molecule to remain in a globular shape. For the "ends", "middle", and "side" systems, while the portions of the PGG backbone with PTX conjugation are driven to self-assembly, the longer unconjugated regions of the backbone are free to move about.

Overall, the results show that the spatial PTX arrangement significantly influences the flexibility of a PGG−PTX molecule, but the PTX loading fraction does not have a marked effect on the flexibility.

Therapeutic Implications of Properties of a PGG−PTX Molecule. Researchers have argued that the ability of a cancer therapeutic to reach tumors may be influenced by properties such as shape, size, and flexibility. In terms of shape, there has been increasing evidence on the benefits of cylindrical and filamentous nanoparticles over their spherical counterparts, such as prolonged blood circulation half-life and improved adhesion and accumulation to fenestrae of tumor endothelia.[6,7] (For this study, the cylindrical shape is considered to be structurally analogous to the filamentous shape.) Such advantages are more likely to be associated with concentrated PGG−PTX solutions rather than dilute PGG−PTX solutions, since filaments are more common in concentrated conditions. However, the filamentous "ends", "middle", and "side" molecules in dilute conditions may also incur a longer circulation half-life and enhanced drug accumulation to tumors. Regarding size, it has been demonstrated that the intracellular signaling pathways implicated in tumor cell function can be activated by nanoparticles of 2−100 nm.[8] The R_g values of ∼3−5 nm for the significant, unique characteristic PGG−PTX conformations confirm that all PGG−PTX molecules are capable of conferring this ability, regardless of PTX loading fraction, spatial PTX arrangement, or solution concentration. Finally, provided the speculation that higher flexibility can increase interactions of nanoparticles to its surrounding biological environment,[9] PGG−PTX molecules at lower PTX loading fractions are most likely to enhance binding to tumors cells.

The implication of these results is that PGG−PTX molecules are primarily filamentous and fairly inflexible in their vial form prior to intravenous administration. During the ADME process, the PGG−PTX concentration will become more dilute, at which the shape of certain PGG−PTX molecules—ones with uniform PTX arrangements—become more globular, while the molecules with more dense PTX arrangements maintain their filamentous morphology. In other words, the "ends", "random", and "side" molecules are likely to confer longer circulation half-life and higher tumor accumulation than the "even", "random", and "clusters" molecules. Moreover, out of the "ends", "random", and "side" molecules, the ones at lower PTX loading fractions, are more likely to effectively bind to surfaces of tumor cells. Once bound to tumor cells, these molecules are also likely to trigger functions such as cell apoptosis, since their size falls within the 2−100 nm range. In all, the "ends", "middle", and "side" PGG−PTX molecules at f_{PTX} = 0.18 and 0.24 in dilute conditions are the most therapeutically promising based on their shape, size, and flexibility.

■ CONCLUSIONS

The goals of this study were two-fold: (1) to develop an insight into possible structural conformations of PGG−PTX and (2) to demonstrate computer simulations as a method to provide insight on the physicochemical properties of anticancer therapeutics that are tedious or difficult to determine experimentally. To suggest conformations of PGG−PTX that may be useful in biological testing, a library of eighteen coarse-grained models of PGG−PTX varying in the PTX loading

fraction (f_{PTX} = 0.18, 0.24, and 0.37) and spatial PTX arrangement (uniform, "even" and "random"; clustered, "clusters" and "ends"; concentrated, "ends" and "side") were constructed. The simulation box size was manipulated to induce dilute and concentrated solutions; molecular dynamics simulations were run for an effective time of 4 μs; and RMSD clustering was used to analyze the conformations. Results show that, in concentrated conditions, each PGG−PTX conformation is affected not only by spatial PTX arrangement and PTX loading fraction but also by periodic interactions with adjacent conformations, unlike dilute conditions, where the conformation is affected only by spatial PTX arrangement and PTX loading fraction. Overall, we demonstrate that the PTX loading fraction and spatial PTX arrangement can be exploited to control the morphology of a PGG−PTX molecule in dilute and concentrated conditions.

■ ASSOCIATED CONTENT

Ⓢ Supporting Information

Tables depicting description of RMSD clustering under dilute and concentrated conditions and local densities of PGG−PTX molecules under dilute and concentrated conditions. Sample calculation of local density of a PGG−PTX molecule under dilute and concentrated conditions. Figures depicting abstract representation of the spatial PTX arrangements on the PGG backbone, sample relationship between the RMSD cutoff length and number of clusters for a PGG−PTX molecule, representative conformations of certain PGG−PTX molecules, and minimum periodic distance trajectories for PTX residues of PGG−PTX molecules. This material is available free of charge via the Internet at http://pubs.acs.org.

■ AUTHOR INFORMATION

Corresponding Author

*University of California, San Diego, Department of Bioengineering, La Jolla, CA 92093. E-mail: dgough@ucsd.edu. Phone: 858-822-3446. Fax: 858-534-5722.

■ ACKNOWLEDGMENTS

Financial support for this work was provided by the UC Discovery Grant bio06-10568 and the Nitto Denko Technical (NDT) Corporation. L.Y. is a full-time employee of NDT, and S.B.H. and D.A.G. serve as consultants for NDT on an arrangement approved by the UCSD Conflict of Interest Committee. The authors acknowledge M. Fajer for excellent technical input and J. A. McCammon and the National Biomedical Computation Resource (Grant P41RR008605) for the supercomputing resources.

■ REFERENCES

(1) Ferrari, M. Cancer nanotechnology: opportunities and challenges. *Nat. Rev.* **2005**, *5*, 161−171.
(2) Ferrari, M. Beyond drug delivery. *Nat. Nanotechnol.* **2008**, *3*, 131−132.
(3) Decuzzi, P.; Pasqualini, R.; Arap, W.; Ferrari, M. Intravascular delivery of particulate systems: does geometry really matter? *Pharm. Res.* **2009**, *26*, 235−243.
(4) Duncan, R. The dawning era of polymer therapeutics. *Nat. Rev. Drug Discovery* **2003**, *2*, 347−360.
(5) Nishiyama, N. Nanocarriers shape up for long life. *Nat. Nanotechnol.* **2007**, *2*, 203−204.
(6) Geng, Y.; Dalhaimer, P.; Cai, S.; Tsai, R.; Tewari, M.; Minko, T.; Discher, D. E. Shape effects of filaments versus spherical particles in flow and drug delivery. *Nat. Nanotechnol.* **2007**, *2*, 249−255.
(7) Srinivas, G.; Shelley, J. C.; Nielson, S. O.; Discher, D. E.; Klein, M. L. Simulation of diblock copolymer self-assembly, using a coarse-grain model. *J. Phys. Chem. B* **2004**, *108*, 8153−8160.
(8) Jiang, W.; Kim, B. Y.; Rutka, J. T.; Chan, W Nanoparticle-mediated cellular response is size-dependent. *Nat. Nanotechnol.* **2008**, *3*, 145−150.
(9) Takeoka, S. Rolling properties of rGPIbα-conjugated phospholipid vesicles with different membrane flexibilities on vWf surface under flow conditions. *Biochem. Biophys. Res. Commun.* **2002**, *296*, 765−770.
(10) Pujol, J. L., Phase II study of carboplatin and weekly paclitaxel as first line treatment of elderly patients with non-small cell lung cancer. In *Clinical Study Report for Study CA139-368*; Bristol-Myers Squibb: Montpellier, France, 2005.
(11) Piccart, M. J.; Bertelsen, K.; James, K.; Cassidy, J.; Mangioni, C.; Simonsen, E.; Stuart, G.; Kaye, S.; Vergote, I.; Blom, R.; Grimshaw, R.; Atkinson, R. J.; Swenerton, K. D.; Trope, C.; Nardi, M.; Kaern, J.; Tumolo, S.; Timmers, P.; Roy, J. A.; Lhoas, F.; Lindvall, B.; Bacon, M.; Birt, A.; Andersen, J. E.; Zee, B.; Paul, J.; Baron, B.; Pecorelli, S. Randomized intergroup trial of cisplatin-paclitaxel vs. cisplatin-cyclophosphamide in women with adavnced epithelial ovarian cancer. *J. Natl. Cancer Inst.* **2000**, *92*, 699−708.
(12) Yoshida, T., Rollover study of weekly paclitaxel (BMS-181339) in patients with advanced breast cancer. In *Clinical Study Report for Study CA139-387*; Bristol-Myers Squibb: Tokyo, Japan, 2009.
(13) Sohn, J. J.; Jin, J. I.; Hess, J.; Jo, B. W. Polymer prodrug approaches applied to paclitaxel. *Polym. Chem.* **2010**, *1*, 778−792.
(14) Wang, X.; Zhao, G.; Van, S.; Yu, L. Polymer paclitaxel conjugates and methods for treating cancer. 2009, Patent number: US20090226393, 127. Assignee: Nitto Denko Technical Corporation, 501 Via Del Monte, Oceanside, CA.
(15) Wang, X.; Zhao, G.; Van, S.; Jiang, N.; Yu, L.; Vera, D.; Howell, S. B. Pharmacokinetics and tissue distribution of PGG-paclitaxel, a novel macromolecular formulation of paclitaxel, in nu/nu mice bearing NCI-460 lung cancer xenografts. *Cancer Chemother. Pharmacol.* **2009**, *65*, 515−526.
(16) Van, S.; Das, S. K.; Wang, X.; Feng, Z.; Jin, Y.; Hou, Z.; Chen, F.; Pham, A.; Jiang, N.; Howell, S. B.; Yu, L. Synthesis, characterization, and biological evaluation of poly(L-gamma-glutamyl-glutamate)-paclitaxel nanoconjugate. *Int. J. Nanomed.* **2010**, *5*, 825−837.
(17) Vauthier, C.; Fattal, E.; Labarre, D. From Polymer Chemistry and Physicochemistry to Nanoparticulate Drug Carrier Design and Applications. In *Tissue Engineering and Novel Delivery Systems*; Yaszemski, M. J., Ed.; Marcel Dekker: New York, 2004; Vol. *1.1*, Chapter 26.
(18) Schames, J.; Henchman, R. H.; Siegel, J. S.; Sotriffer, C. A.; Ni, H.; McCammon, J. A. Discovery of a novel binding trench in HIV integrase. *J. Med. Chem.* **2004**, *47*, 1879−1881.
(19) Amaro, R. E.; Schnaufer, A.; Interthal, H.; Hol, W.; Stuart, W. D.; McCammon, J. A. Discovery of drug-like inhibitors of an essential RNA-editing ligase in trypanosoma brucei. *Proc. Natl. Acad. Sci. U.S.A.* **2008**, *106*, 17278−17283.
(20) Zewail, A. H. Computer-aided drug discovery: physics-based simulations from the molecular to the cellular level. In *Physical Biology: From Atoms to Medicine*; Zewail, A. H., Ed.; World Scientific Publishing: 2008; pp 401−410.
(21) Peng, L. X.; Ivetac, A.; Chaudhari, A. S.; Van, S.; Zhao, G.; Yu, L.; Howell, S. B.; McCammon, J. A.; Gough, D. A. Characterization of a clinical polymer-drug conjugate using multiscale modeling. *Biopolymers* **2010**, *93*, 936−951.
(22) Lindahl, E.; Hess, B.; van der Spoel, D. GROMACS 3.0: A package for molecular simulation and trajectory analysis. *J. Mol. Model.* **2001**, *7*, 306−317.
(23) Marrink, S. J.; de Vries, A. H.; Mark, A. E. Coarse-grained model for semi-quantitative lipid simulations. *J. Phys. Chem. B* **2004**, *108*, 750−760.

(24) Marrink, S. J.; Rissalada, J. H.; Yefimov, S.; Tieleman, D. P.; de Vries, A. H. The MARTINI force field: coarse-grained model for biomolecular simulations. *J. Phys. Chem. B* **2007**, *111*, 7812−7824.
(25) Monticelli, L.; Kandasamy, S. K.; Periole, X.; Larson, R. G.; Tieleman, D. P.; Marrink, S. J. The MARTINI coarse-grained force field: extension to proteins. *J. Chem. Theory Comput.* **2008**, *4*, 819−834.
(26) Peng, L. X.; Das, S. K.; Yu, L.; Howell, S. B.; Gough, D. A. Coarse-grained modeling study of nonpeptide RGD ligand density and PEG molecular weight on the conformation of poly(γ-glutamyl-glutamate) paclitaxel conjugates. *J. Mol. Mod.* **2011**, *17*, 2973−2987.
(27) Humphrey, W.; Dalke, A.; Schulten, K. VMD - Visual Molecular Dynamics. *J. Mol. Graphics* **1996**, *14*, 33−38.
(28) McQuarrie, D. A. Statistical Mechanics; University Science Books: Sausolito, CA, 2000.